 doi:10.20944/preprints201806.0354.v1

In-situ synthesize of graphene-Mn_3O_4 nanocomposites for high-rate pseduocapacitive electrodes

Danfeng Qiu[1,*], Xiao Ma[1], Jingdong Zhang[1], Bin Zhao[2], Zixia Lin[2]

[1] Key Laboratory of Radar Imaging and Microwave Photonics (Nanjing Univ. Aeronaut. Astronaut.), Ministry of Education, College of Electronic and Information Engineering, Nanjing University of Aeronautics and Astronautics, Nanjing, 210016, China; dfqiu@nuaa.edu.cn (D.Q.); 2792359285@qq.com (X.M.); zhangjd@nuaa.edu.cn (J.Z.)

[2] National Laboratory of Microstructures and School of Electronic Science and Engineering, Nanjing University, Nanjing, China; binzcaptain@gmail.com (B.Z.); 267319441@qq.com (Z.L.)

* Correspondence: dfqiu@nuaa.edu.cn;

Abstract: Mn_3O_4 /graphene nanosheets (GNS) composites serve as very excellent electrode materials for supercapacitors. They can fully combine the advantages of two materials such as graphene and metal oxide. Meanwhile, they can improve not only the specific energy and specific power of the materials, but also the cyclic stability of the materials. The results of the cyclic voltammetry and constant current charge discharge test on the composite electrode material have shown that the Mn_3O_4 /GNS powder sample has good capacitive performance. When the scanning rate is 5~50mV, the specific capacity retention rate of the composite electrode is 80.3% and 88% respectively. Mn_3O_4 nanoparticles, with the highest ratio of network coated GNS, exhibit a specific capacitance value of 957.6 F g^{-1} at a current density of 2 A g^{-1} in 1 M Na_2SO_4 solution. Besides, its network structure demonstrates high specific capacity and multiplying performance.

Keywords: Graphene; Mn_3O_4; Nanocomposites; Energy storage and conversion; Supercapacitors

1. Introduction:

Due to the shortage of mineral energy and the increasingly serious environmental problems, scholars start to attach more attention on high performance energy storage and conversion functional materials and devices [1-3]. Supercapacitor, as a new type of energy storage element, has large capacity, high energy, wide working temperature range and long service life, can generate large current within a short term and has

Preprints (www.preprints.org) | NOT PEER-REVIEWED | Posted: 22 June 2018 doi:10.20944/preprints201806.0354.v1

become a research hotspot in recent years [4-7]. Metal oxide electrodes have been paid more and more attention because the rapid reversible redox reaction can penetrate into the electrode while the energy can be stored in the three-dimensional space to improve the energy density [8-10]. At present, the promising metal oxide electrode materials are mainly MnOx (x =1, 2, 3/2, 4/3) [11-15], NiO[16], Co_3O_4[17], V_2O_5[18] and RuO_2[19].

In all kinds of pseudopotential electrode materials, ruthenium oxide (RuO_2) has been widely studied because of its good conductivity, rapid reversible redox reaction and high specific capacity [20, 21]. However, due to its price price and toxic features, it has not been widely applied. Therefore, finding a cheap alternative material becomes rather urgent. Manganese oxide enjoys multiple advantages, such as high theoretical specific capacity (1370 F g^{-1} [22, 23]), good environmental compatibility, good oxidation-reduction and charge storage characteristics, high chemical, thermal stability, and low price. It is expected to replace RuO_2 in some fields. Meanwhile, MnOx also enjoys some advantages, such as rich material, low cost and friendly environment. However, its electrical conductivity (10^{-7} ~10^{-8} S cm^{-1}) is quite low, which limits its application in the field of supercapacitor. As the cycle life of a single MnOx is still not ideal yet, there are many carbon materials, such as activated carbon、carbon nanotube, carbon aerogels and graphene etc. have been widely applied to combine with the metal oxides and hence to increase the conductivity of manganese oxide.

Graphene has a unique two-dimensional structure with a single atomic thickness, high specific surface area, excellent electrical and mechanical properties. Therefore, the combination of graphene and Mn_3O_4 can not only improve the electrical and mechanical strength of Mn_3O_4, but also bring greater surface/boundary area to the composite. More electrochemical active sites, therefore, are provided in this way. Manganese oxide loaded with graphene has a good application prospect as the electrode material of supercapacitor. However, the preparation of manganese oxide is very complex. Currently, it is mainly constrained by two aspects, including the immaturity of the process and the high cost.

Preprints (www.preprints.org) | NOT PEER-REVIEWED | Posted: 22 June 2018 doi:10.20944/preprints201806.0354.v1

In this paper, Mn_3O_4/GNS nanocomposites were prepared by thermal decomposition of graphene and manganese nitrate complex. The organic combination of graphene and manganese oxide nanoparticles can fully realize the synergistic effect of double capacitance and pseudo capacitance. The pore structure of electrode materials is an important factor affecting the capacitance performance. Three dimensional porous Mn_3O_4/GNS composites were constructed by thermal decomposition of manganese oxide nanoparticles in situ by three-dimensional porous graphene paper. The three-electrode system exhibits a specific capacitance value of 987.6 F g^{-1} at a current density of 2 A g^{-1} in 1 M Na_2SO_4 solution. Such composite exhibits good cyclic stability with a small loss of 5.2% of maximum capacitance over 2000 consecutive cycles.

2. Experimental

GO was synthesized from natural graphite powders (universal grade, 99.985%) based on the Hummers' method with slight modifications [24, 25]. The as-prepared GO was stripped for 3 minutes in air at 300 °C, and then treated for 3 hours in Ar protection at 900 °C. Then, GNS was obtained. In the synthesis of typical Mn_3O_4/GNS nanocomposites, 537 mg of Mn $(NO_3)_2$ aqueous solution (50%) was mixed with 50 ml ethanol. Besides, 28 mg of GNS was added to the solution for 15 minutes. The suspension is mixed with a magnetic stirrer in the hood combined with the continuous evaporation of the ethanol in the solution. Dry Mn $(NO_3)_2$ / GNS composites were collected and treated at 200 °C for 10 h, and Mn $(NO_3)_2$ was converted to Mn_3O_4. The relevant mechanisms can be explained as follows:

$$3Mn(NO_3)_2 \rightleftarrows 3Mn_3O_4 + 6NO \quad (1)$$

Based on weight, there is about 80% of Mn_3O_4/GNS is Mn_3O_4. During the control experiments, a $Mn(NO_3)_2$ aqueous solution (50%) was heated in the air under 200 °C for 10 h to prepare the simplex Mn_3O_4 sample. The obtained samples were explored via TEM, namely transmission electron microscopy, SEM, namely scanning electron microscopy and XRD, namely X-ray diffraction. Base materials (10 wt.%), which were mixed with N, N di-methyl-acetamide (~10 ml). were used to fabricate

Preprints (www.preprints.org) | NOT PEER-REVIEWED | Posted: 22 June 2018 doi:10.20944/preprints201806.0354.v1

the Mn_3O_4/GNS electrode. Afterwards, the final mixture obtained was stirred under the room temperature for around 24h using a magnetic stirrer (1200 rpm). Subsequently, a think graphite sheet (specific area of 1 × 1 cm^2) was used to coat the final product. The electrodes being prepared later got dried under 60 °C in the hot air oven for around 3h. For the fabricated electrodes, there was around 1.2 mg cm^{-2} mass loading of active materials over the graphite sheet. The same electrochemically active material/binder (PVDF)/conductive carbon ratio (80:10:10) was also used for the preparation of pure Mn_3O_4 and GNS for the control experiment and hence to make an accurate electrochemical properties of the resultant electrodes.

3. Results and Discussion

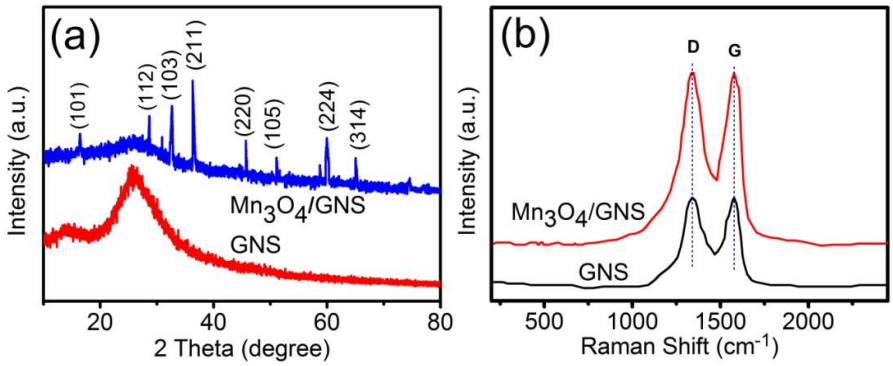

Fig.1 . (a) XRD and b) Raman characterizations of GNS and Mn_3O_4/GNS samples.

It can be seen from the XRD analysis chart of the composite powder in Fig. 1a that the major components of graphene and GNS/ Mn_3O_4 have low crystallinity. The diffraction peaks occurring on the all the reflections of the samples are consistent with the standard pattern of the tetragonal Mn_3O_4 (JCPDS file no. 80-0382). There was none other impurity or phase being found in these patterns. For the multiplayer graphene of the GNS sample, the broad peak at around 25 °C was a kind of diffraction peak. There are two typical peaks of both samples which are at around 1350 and 1585 cm^{-1} being assigned to D and G brands of graphene correspondingly, suggesting that there were a multitude of defects in the GNS.

Fig. 2a and 2b show that there are obvious lamellar structures and wrinkles at the edge of the graphene sheet. The natural flexural lamellar structure of graphene and the formed fold structure increase the specific surface area of the prepared three

Preprints (www.preprints.org) | NOT PEER-REVIEWED | Posted: 22 June 2018 doi:10.20944/preprints201806.0354.v1

dimensional channel interworking material, providing a good condition for the load of Mn_3O_4 nanoparticles.

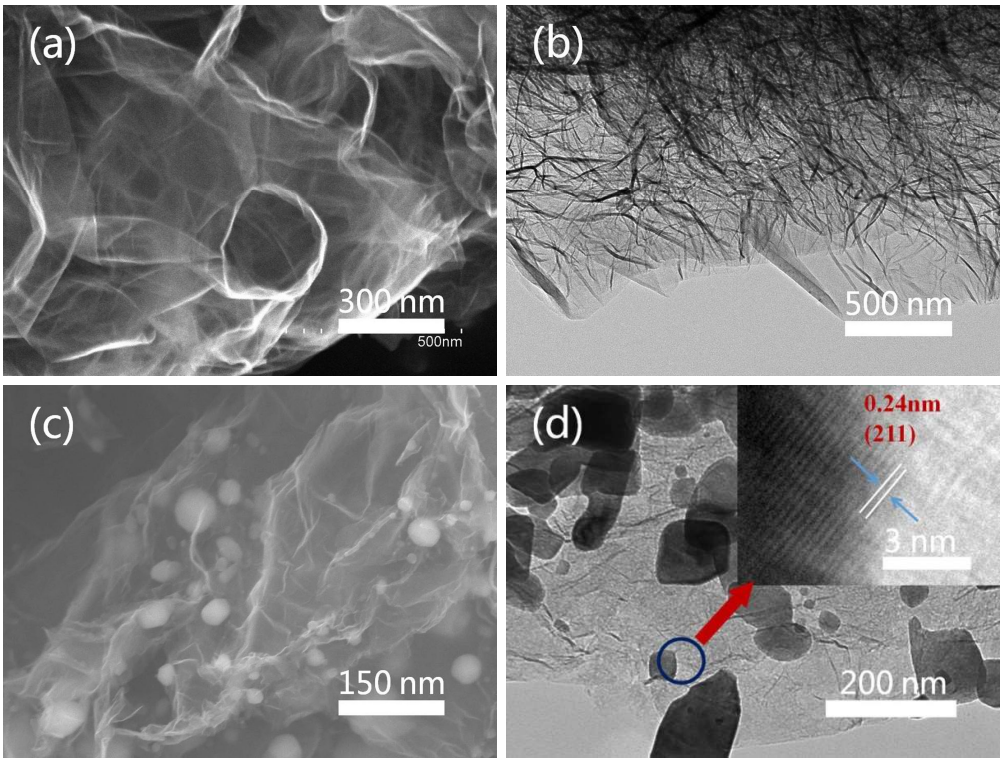

Fig. 2. SEM (a) and TEM (b) images GNS; SEM (c) and TEM (d) images of Mn_3O_4/GNS.

Besides, according to fig. 2c and 2d, it can be seen that the size of Mn_3O_4 is around 20-100 nm. Mn_3O_4 nanoparticles are dispersed on the surface of the graphene to form an interconnected junction. Meanwhile, for the trip of manganese oxide crystals, the graphene is of great importance. The pore structure of the 3D network skeleton effectively limits the size of the manganese oxide nanoparticles. At the same time, the pore of the graphene has been further expanded through the gas generated from the decomposition of manganese nitrate. The synergistic effect between graphene and manganese oxide was obvious. This not only improves the conductivity of materials, but also accelerates the diffusion of anion and cation.

Fig. 3a shows the cyclic voltammetry (CV) curves of as prepared samples of Mn_3O_4/GNS nanocomposites. The redox peaks appear in the cyclic voltammetry curves of Mn_3O_4/GNS are near O.23 and 0.45 V, indicating that the capacitor is mainly a pseudopotential, which mainly stores charge by two-dimensional and quasi

Preprints (www.preprints.org) | NOT PEER-REVIEWED | Posted: 22 June 2018 doi:10.20944/preprints201806.0354.v1

two-dimensional Faraday reaction on the surface of the electrode. There is a weak redox peak in the cyclic voltammetry curve of Mn_3O_4/GNS. The current response becomes faster when there is a change occurring over the potential of the end potential, indicating that the reversibility of the material is better. The size of the area enclosed by the cyclic voltammetry curves of the Mn_3O_4/GNS materials shows the maximum capacitance of Mn_3O_4/GNS, indicating that the manganese and nickel oxide in the composite have a direct effect on the capacitance.

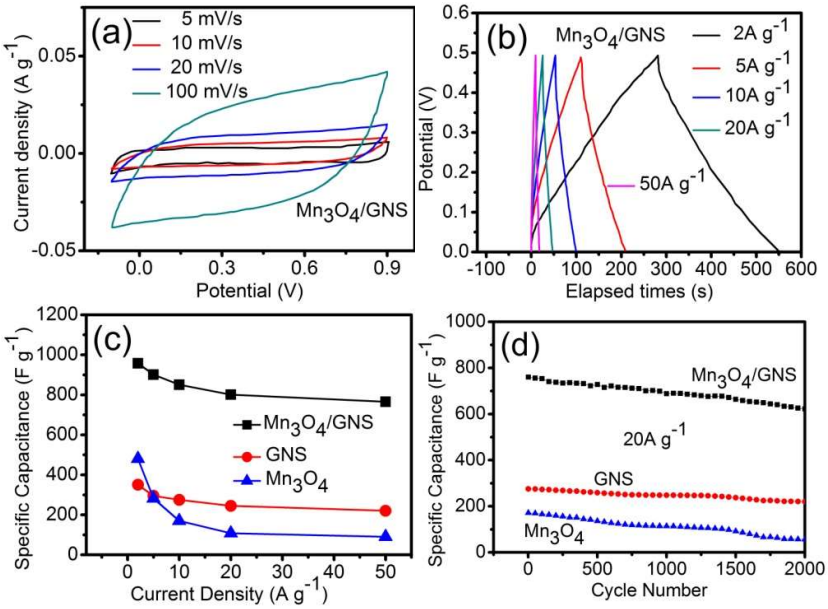

Fig. 3. (a) CV curves of Mn_3O_4/GNS with different scan rates; (b) charge/discharge curves of Mn_3O_4/GNS at various current densities; (c) the specific capacitance of composites with different current densities; (d) cycling performances of composites at current density of 20 mA g^{-1}.

The specific capacitance of Mn_3O_4/GNS nanocomposites is larger and reversible. Fig. 3b presents the charging and discharging curves of Mn_3O_4/GNS nanocomposites. The calculated specific capacitance at is 957.6, 905.2, 854.6, 802.3,765.2 F g^{-1} at the current density of 2, 5, 10, 20, 50 A g^{-1} respectively, which are proved by a large number of cyclic tests (Fig. 3c). After 1000 cycles of charge and discharge under current density of 20 A g^{-1}, the specific capacitance did not fail significantly, which was still 763.8 F g^{-1}. That suggests that it retained 95.2% of the original activity. This is due to the synergistic effect of Mn_3O_4 and graphene during the electrochemical testing, which inhibits the loss of specific capacitance because of the large

Preprints (www.preprints.org) | NOT PEER-REVIEWED | Posted: 22 June 2018 doi:10.20944/preprints201806.0354.v1

crystallization of the other side. In light of this, regardless of the increase of specific capacitance or the prolongation of cycle life, the combination of Mn_3O_4 and graphene has played a good role during the promotion.

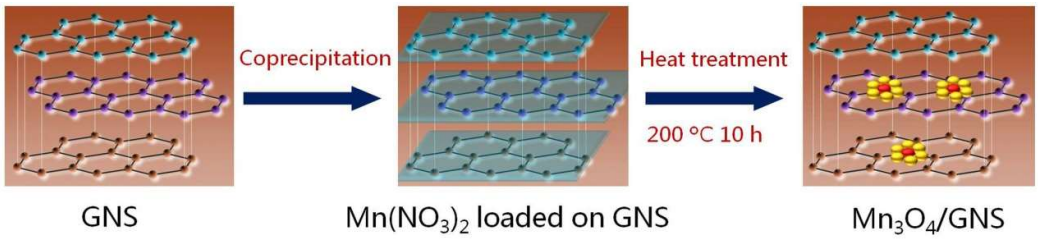

Fig. 4. Schematic illustration of the Mn_3O_4/GNS nanocomposite material.

From Fig. 3d, the sample Mn_3O_4/GNS has a second-highest capacity retention rate in 3 samples while the capacity of the sample is the highest. The sample of graphene has the highest capacity retention rate. However, the capacity is far lower than that of the Mn_3O_4/GNS sample. This is due to the supporting effect of graphene on the overall morphology of the powder, making the composite powder form a good network structure, and the specific surface area and mesoporous porous content of the powder are greatly improved.

The synthesis mechanism of Mn_3O_4/GNS nanocomposites is shown in Fig. 4. By means of solution coprecipitation, manganese nitrate can uniformly adhere to the surface of graphene. Then, the thermal decomposition was conducted, decomposing the manganese nitrate into Mn_3O_4 nanocomposites. This method of in-situ thermal decomposition ensures that Mn_3O_4 nanoparticles can be firmly embedded in the surface and channel of graphene to achieve good electrical contact and thus to improve the electrochemical properties of manganese oxide in the process of charge and discharge.

4. Conclusions

Mn_3O_4/GNS nanocomposites were synthesized by liquid phase codeposition. Afterwards, the thermal decomposition was conducted. It can be found through the SEM and XRD analysis that the obtained compound is rather complex. It has been shown from the electrochemical tests that graphene and Mn_3O_4 composite electrodes have better electrochemical capacitance than graphene. In the constant current charge

 doi:10.20944/preprints201806.0354.v1

discharge test, the specific capacitance of the composite material is about 760 F g^{-1} under the high current charge while the discharge is up to 20 A g^{-1}. Meanwhile, the specific capacitance retention rate of the 2000 cycles is as high as 95%. The CV curve of the composites were approximately rectangular, indicating that the composites had good reversibility.

Acknowledgments: This work was supported by the National Key R&D Program of China under Grant 2017YFB0502700, the National Natural Science Foundation of China (No. 61471195), and the Fundamental Research Funds for the Central Universities (Nos. NZ2016105, NJ20150017 and NS2014040), partially by the National Defense Pre-Research Foundation of China (No.6140413020116HK02001).

Author Contributions: Danfeng Qiu and Jingdong Zhang conceived and designed the experiments; Xiao Ma performed the experiments; Danfeng Qiu and Bin Zhao analyzed the data, reviewed and edited this manuscript; Zixia Lin contributed reagents/materials/analysis tools; Danfeng Qiu and Xiao Ma wrote the paper.

Conflicts of Interest: The authors declare no conflict of interest.

References

1. Gu,W.; Yushin, G. Review of nanostructured carbon materials for electrochemical capacitor applications: Advantages and limitations of activated carbon, carbide-derived carbon, zeolite-templated carbon, carbon aerogels, carbon nanotubes, onion-like carbon, and graphene. Wiley Interdiscip. Rev. Energy Environ. **2014**, 3, 424–473.
2. Armand, M.; Tarascon, J.M.; Building better batteries, Nature. **2008**, 451, 652–657.
3. Peng, X.; Peng, L.; Wu, C.; Xie, Y. Two dimensional nanomaterials for flexible Supercapacitors. Chem. Soc. Rev. **2014**, 43, 3303–3323.
4. Zheng, S.; Li, X.; Yan, B.; Hu, Q.; Xu, Y.; Xiao, X.; Xue, H.; Pang, H. Transition-Metal (Fe, Co, Ni) Based Metal-Organic Frameworks for Electrochemical Energy Storage. Adv. Energy Mater. **2017**, 7, 1602733.

5. Winter, M.; Brodd, R.J. What are batteries, fuel cells, and supercapacitors? Chem. Rev. **2004**, 104, 4245–4269.
6. Yu, G.; Xie, X.; Pan, L.; Bao, Z.; Cui, Y. Hybrid nanostructured materials for high-performance electrochemical capacitors. Nano Energy **2013**, 2, 213–234.
7. Jang, H.; Park, Y.J.; Chen, X.; Das, T.; Kim, M.-S.; Ahn, J.-H. Graphene-based flexible and stretchable electronics. Adv. Mater. **2016**, 28, 4184–4202.
8. Wei,W.; Cui, X.; Chen,W.; Ivey, D.G. Manganese oxide-based materials as electrochemical supercapacitor electrodes. Chem. Soc. Rev. **2011**, 40, 1697–1721.
9. Xiong, P.; Ma, R.; Sakai, N.; Bai, X.; Li, S.; Sasaki, T. Redox Active Cation Intercalation/Deintercalation in Two-dimensional layered MnO2 nanostructures for high-rate electrochemical energy storage. ACS Appl. Mater. Interfaces **2017**, 9, 6282–6291.
10. Devaraj, S.; Munichandraiah, N. Effect of crystallographic structure of MnO2 on its electrochemical capacitance properties. J. Phys. Chem. C **2008**, 112, 4406–4417.
11. Omomo, Y.; Sasaki, T.; Zhou, L.; Watanabe, M. Redoxable nanosheet crystallites of MnO2 derived via delamination of a layered manganese oxide. J. Am. Chem. Soc. **2003**, 125, 3568–3575.
12. Huang, W.X.; Li, Jun. ; Xu. Y.H. Nucleation/Growth Mechanisms and Morphological Evolution of Porous MnO2 Coating Deposited on Graphite for Supercapacitor. Materials **2017**, 10, 1205.
13. Xiong, P.; Ma, R.; Sakai, N.; Bai, X.; Li, S.; Sasaki, T. Redox Active Cation Intercalation/Deintercalation in Two-dimensional layered MnO2 nanostructures for high-rate electrochemical energy storage. ACS Appl. Mater. Interfaces **2017**, 9, 6282–6291.
14. Devaraj, S.; Munichandraiah, N. Effect of crystallographic structure of MnO2 on its electrochemical capacitance properties. J. Phys. Chem. C **2008**, 112, 4406–4417.
15. Shao, J.; Zhou, X.; Liu, Q.; Zou, R.; Li, W.; Yang, J.; Hu, J. Mechanism analysis of the capacitance contributions and ultralong cycling-stability of the isomorphous MnO2@MnO2 core/shell nanostructures for supercapacitors. J. Mater. Chem. A **2015**, 3, 6168–6176.
16. Wang, Y.G.; Xia, Y.Y. Electrochemical capacitance characterization of NiO with ordered mesoporous structure synthesized by template SBA-15. Electrochim. Acta **2006**, 51, 3223–3227.
17. Ning, J.F.; Zhang, T.Y.; He, Y.; Jia, C.P.; Saha, P. Cheng, Q.L. Co_3O_4@CoS Core-Shell Nanosheets on Carbon Cloth for High Performance Supercapacitor Electrodes. Materials **2017**, 10, 608.

18. Saravanakumar, B.; Purushothaman, K.K.; Muralidharan, G. Fabrication of two-dimensional reduced graphene oxide supported V2O5 networks and their application in supercapacitors. Mater. Chem. Phys. 2016, 170 (Suppl. C), 266–275.
19. Gigot, A.; Fontana, M.; Pirri, C.F.; Rivolo, Paola, Graphene/Ruthenium Active Species Aerogel as Electrode for Supercapacitor Applications. Materials **2018**, 11, 57.
20. Kim, Y.L.; Choi, H.A.; Lee, N.S.; Son, B.; Kim, H.J.; Baik, J.M.; Lee, Y.; Lee, C.; Kim, M.H. RuO2-ReO3 composite nanofibers for efficient electrocatalytic responses. Phys. Chem. Chem. Phys. **2015**, 17, 7435–7442.
21. Wu, Z.S.;Wang, D.W.; Ren,W.; Zhao, J.; Zhou, G.; Li, F.; Cheng, H.M. Anchoring hydrous RuO_2 on graphene sheets for high-performance electrochemical capacitors. Adv. Funct. Mater. **2010**, 20, 3595–3602.
22. Tian, Y.Y.; Li, D.W.; Liu, J.L.; Wang, H.; Zhang, J.F.; Zheng, Y.Q.; Liu, T.H.; Hou, S.F. Facile Synthesis of Mn3O4 Nanoplates-Anchored Graphene Microspheres and Their Applications for Supercapacitors. Electrochim. Acta **2017**, 257, 155–164.
23. Shah, H.U.; Wang,, F.P.; Javed, M.S.; Shaheen, Nu.; Saleem, M. Li, Y. Hydrothermal synthesis of reduced graphene oxide-Mn3O4 nanocomposite as an efficent electrode materials for supercapacitors. Ceramics International **2018**, 44, 3580–3584.
24. Hummers, W.S.; Offeman, R.E. Preparation of graphitic oxide. J. Am. Chem. Soc. **1958**, 80, 1339–1339.
25. Du, Q.L.; Zheng, M.B.; Zhang, L.F.; Wang, Y.W.; Chen, J.H.; Xue, L.P.; Dai, W.J.; Ji, G.B.; Cao, J.M. Electrochim. Acta **2010**, 55, 3897–3903.